

INTERACTION OF OIL WITH SEA ICE

by

Seelye Martin

School of Oceanography
University of Washington

Outer Continental Shelf Environmental Assessment Program
Final Report
Research Unit 87

May 1982

TABLE OF CONTENTS

List of Figures	5
Abstract	7
1. Introduction	8
2. Ocean and Ice Processes	8
3. Ice Band Properties	14
4. Oil in the MIZ	18
Appendices :	
1. Physical Oceanographic Investigations in the Bering Sea Marginal Ice Zone	19
2. The Movement and Decay of Ice Edge Bands in the Bering Sea	75
3. On Some Possible Interactions Between Internal Waves and Sea Ice in the Marginal Ice Zone	125
4. The Bering Sea Ice Cover during March 1979: Comparison of Surface and Satellite Data with the NIMBUS-7 SMMR	161

LIST OF FIGURES

- Figure 1. Observation area and location of moored current meter **BC22**.
- Figure 2. Vertical distribution of temperature across the central Bering Sea shelf, approximately beneath the ice edge, prior to (upper) and following (lower) a strong, southerly wind event in mid-winter 1981. Figure 2-2 in Appendix 1 shows locations of stations which are included in these two transects. Numbers given are cast numbers.
- Figure 3. Bottom topography in the experimental region.
- Figure 4. Comparison of band motion with currents measured at **BC22**.
- Figure 5. Schematic drawing of the band in cross section.

ABSTRACT

This document constitutes the final report of contract number **NA81RAC00013**. The document is composed of a summary introduction, plus four Appendices. Appendix 1 is a report entitled "Physical oceanographic investigations in the Bering Sea Marginal Ice Zone," by **Robin Muench**. Appendix 2 is a manuscript titled "The movement and decay of ice edge bands in the Bering Sea,"* by Martin, Kauffman, and Parkinson. Together, these two manuscripts describe the oceanographic and sea ice conditions during the mid-winter **1981** SURVEYOR cruise. We also include copies of two related reports in Appendices 3 and 4. The first, a paper entitled "On some possible interactions between internal waves and sea ice in the marginal ice zone," by **Muench, LeBlond, and Hachmeister**, uses the data described in Appendix 1 and 2 to describe possible interactions between internal waves and ice bands in the Bering Sea. The second, "'The Bering Sea ice cover during March 1979: comparison of surface and satellite data with the NIMBUS-7 **SMMR**" describes an all-weather satellite technique for following the evolution of the Bering Sea ice cover.

1. Introduction

The following short report provides both **an** overview **and** a drawing together of the material in the Appendices. Within this section, we will repeat several of the figures **in** the Appendices; and all references will be to work cited in the Appendices. In the following, we first discuss the Bering Sea oceanography, with particular reference to a salinity-temperature front which we feel strongly interacts with the ice edge. We then discuss the nature of the ice edge as revealed from our February-March 1981 cruise; and finally discuss the relevance of our observations to the interaction of oil with the ice edge.

2. Ocean and Ice Processes

Appendix 1 shows in November 1980 and February-March 1981 that a hydrographic structure which was two-layered **in** temperature, salinity, and density, characterized the water of the central Bering Sea shelf. In November, this structure covered the central Bering shelf. **In** February-March, the structure was confined to an 80 km wide front which coincided approximately **with** the ice edge. The cruise results show that the cold, low-salinity upper layer water in the front was continuous in **its** T-S properties **with** the homogeneous water to the north beneath the ice. Similarly, the warmer, more-saline lower layer water was continuous with the Pacific water farther south near the shelf break. To illustrate this front, Figure 1 shows our observational area and the location of the moored current meter **BC22**; and Figure 2a shows the frontal temperature structure preceding a storm.

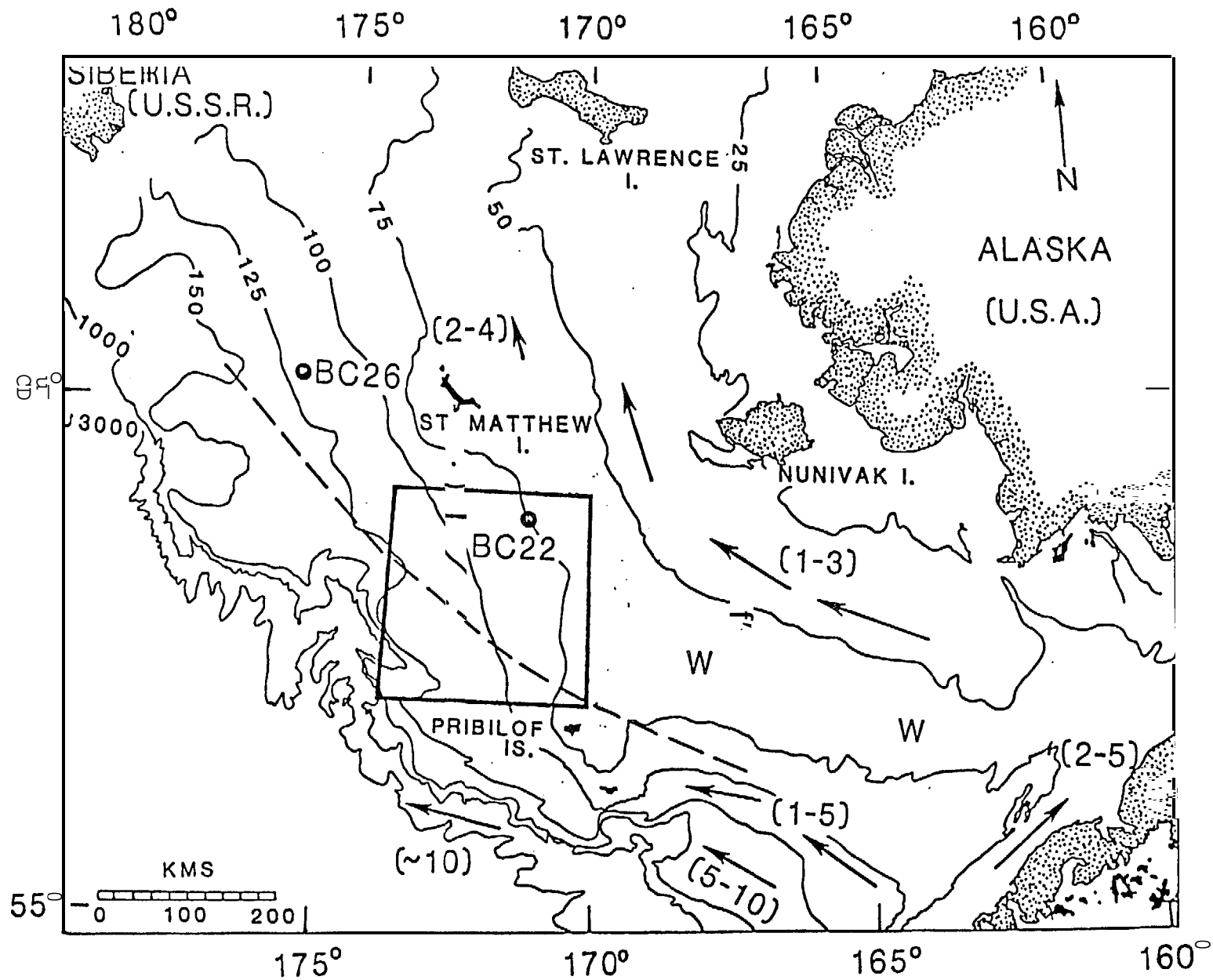


Figure 1. Observation area and location of moored current meter BC22.

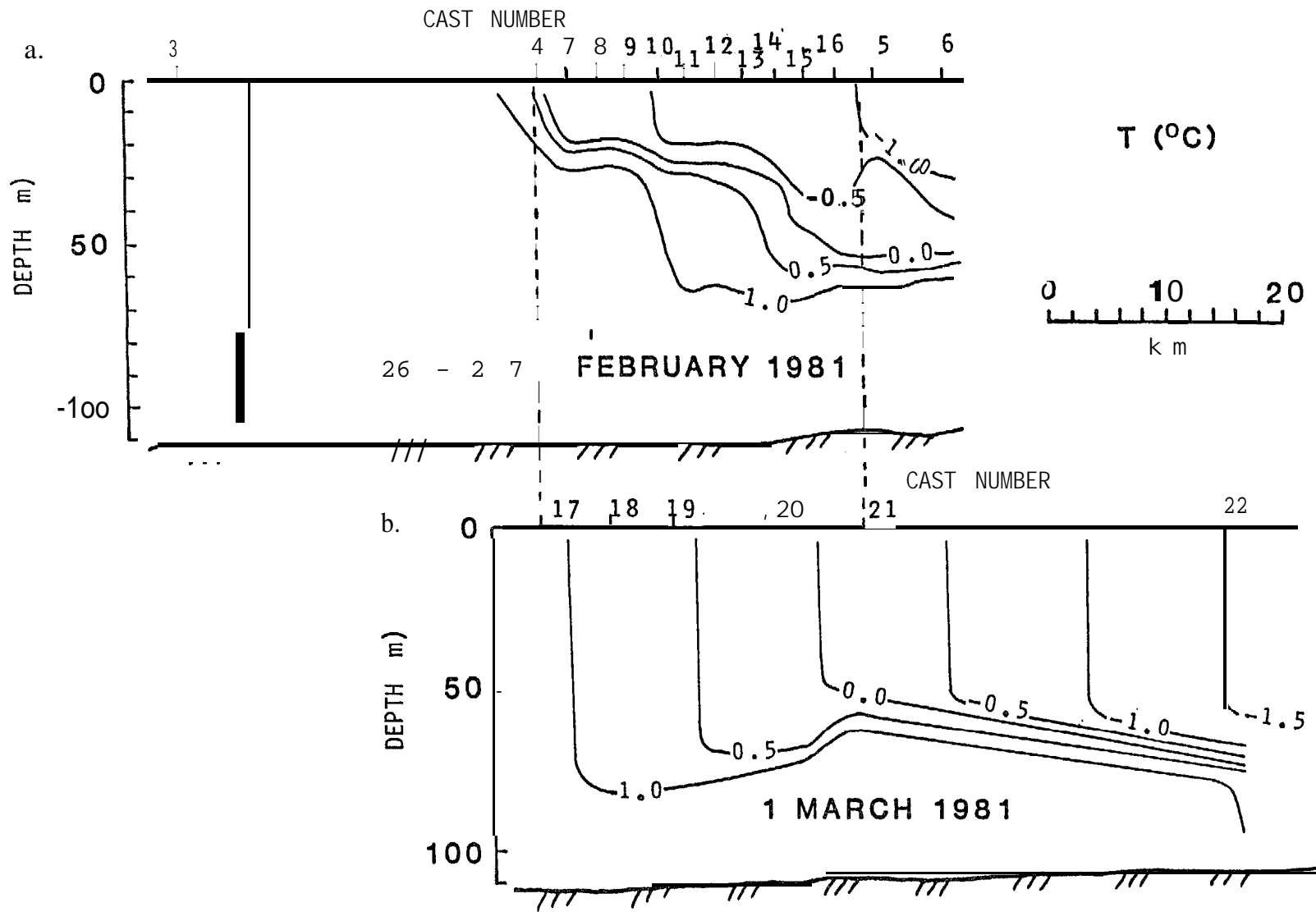


Figure 2. Vertical distribution of temperature across the central Bering Sea shelf, approximately beneath the ice edge, prior to (upper) and following (lower) a strong, southerly wind event in mid-winter 1981. Figure 2-2 in Appendix 1 shows locations of stations which are included in these two transects. Numbers given are cast numbers.

Both our current meters and our **geostrophic** calculations show that this layered front generated a northwest **baroclinic** surface flow with winter surface speeds of about 7 cm s^{-1} . Observed over-winter mean currents at two locations near the ice edge were $2\text{-}3 \text{ cm s}^{-1}$ at 50 m depth, with flow toward the northwest in qualitative agreement with the computed **baroclinic** surface flow and **in** general agreement with the conventional wisdom which presupposes a net north-northwestward flow on the Bering shelf. Fluctuations were superposed on the observed currents and led to periods of reversal. Cross-shelf flow components in particular fluctuated strongly, with the greatest on-shelf flow in mid-winter. Tidal currents were mixed, predominantly diurnal and were $20\text{-}40 \text{ cm s}^{-1}$ east of St. Matthew **Island** and $10\text{-}20 \text{ cm s}^{-1}$ west of it.

Our most interesting observation about this front was its response to a five day storm. During this storm, which caused the **ice** edge to retreat about **100** km, the front did not move with the ice. Rather, while the ice was pushed back into uniformly **cold**, low-salinity water at its freezing point, the comparison of Figure 2b with 2a, which were taken respectively after and before the storm, shows that the two-layer stratification sharpened and deepened, but suffered almost no lateral motion during the storm.

The ice edge started out well to the south on 26 February, then retreated **125 km during the storm** to its maximum retreat position on 3 March. Then given the onset of northeast winds, the ice edge once again advanced southwest to the front, so that by 11 March, the ice edge had returned to its position of 25 February.

From the ship, we observed that when the **ice** was north **of** the front and floating in water **at** its freezing point, the ice did not melt. Instead, we observed grease **ice** growth in the water surrounding the floes. Then, as the northeast winds drove the ice edge back over the front and the surface water temperature rose above the freezing point, the ice began to melt. This melting **cools and** dilutes the surface water and thus contributes to the maintenance of the **front**. As Appendix 2 shows, the melting of ice over the front **is** greatly enhanced through the formation of ice edge bands and their movement over the front. These bands which form at the **ice** edge through mechanisms which we do not yet understand, lie at approximately right angles to the **wind**, are made up of floes measuring approximately 10 m in diameter and 2-4 m **in** thickness, and measure approximately 1 **km** wide by **10** km long. Appendix 2 describes our detailed study of a band, in which we mounted two radar transponders on a band at a distance of 4 **km** apart, then followed the band until it decayed.

Our analysis of the band displacement shows several important facts. **First**, Figure 3 shows a chart of the bottom topography in the experimental region. The point BC22 **is** the current meter mooring; the line "**a**" shows the displacement of a satellite-tracked buoy for the times listed at the end points in **Julian** days **and** GMT, and the line "**b**" **shows** the similar displacement of **our** band. Comparison of the line lengths demonstrate that the band moves about 30% **faster** than the interior ice. Also, under line "**b**", we give the water temperature **in** °C; the temperature increase along the line shows that the band **is** crossing the oceanic **front**. An ice survey described **in** Appendix 2 shows that the satellite-tracked buoy, which was deployed by **Carol** Pease and

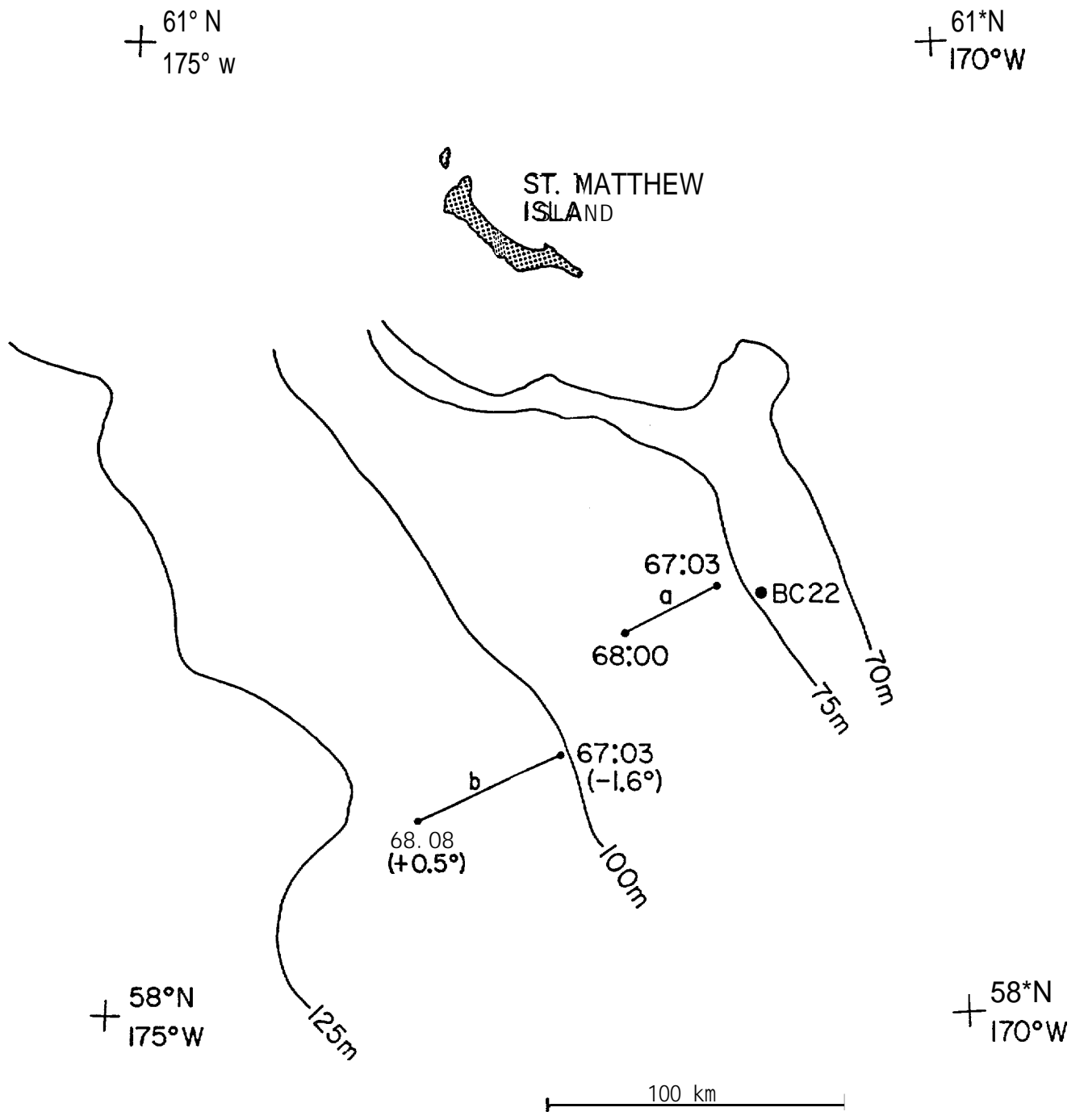


Figure 3. Bottom topography in the experimental region.

will be referred to as 'Pease's station', lay about 80 km **inside** of the ice edge **in** a region of concentrated ice pack. We show below that the cause of the ice band velocity increase relative to Pease's station is the wind-wave radiation stress acting on the band.

3. Ice Band Properties

The ice band has several important small-scale properties relevant to both the large-scale **modelling** of the ice edge, and the ice band behavior. The properties include the following: response of the ice band to tides; the mechanisms for band decay; the band acceleration **by** the wave radiation stress; and the formulation of the air, water, and **Coriolis** stress responsible for **the** ice band motion.

First, we compare in Figure 4 the band **motion** with the currents measured at **BC22**. On Figure 4, the upper two curves show **the** east UC and north \mathbf{v}_C current components from **BC22**; the middle two curves show the ice band velocities \mathbf{u}_I and \mathbf{v}_I ; and the lower two curves show the velocities \mathbf{u}_R and \mathbf{v}_R of the ice relative to the currents. Examination of these curves shows that the rotary tides on the shelf account for most of the oscillations in the band trajectory.

Second, our field observations showed that the ice bands melted according to Figure 5. Figure 5, a schematic drawing of the band in cross section, shows in (a) the initial band configuration; and in (b) the band configuration at a later time. The figure shows that at the upwind band edge the wind-waves are reflected and absorbed, and that the wave agitation breaks up the **large** floes into small pieces. Then, because these **small** pieces are less '**effective** wave absorbers and reflectors than the large floes, they experience a smaller wave radiation stress and thus drift upwind relative to the band to melt in

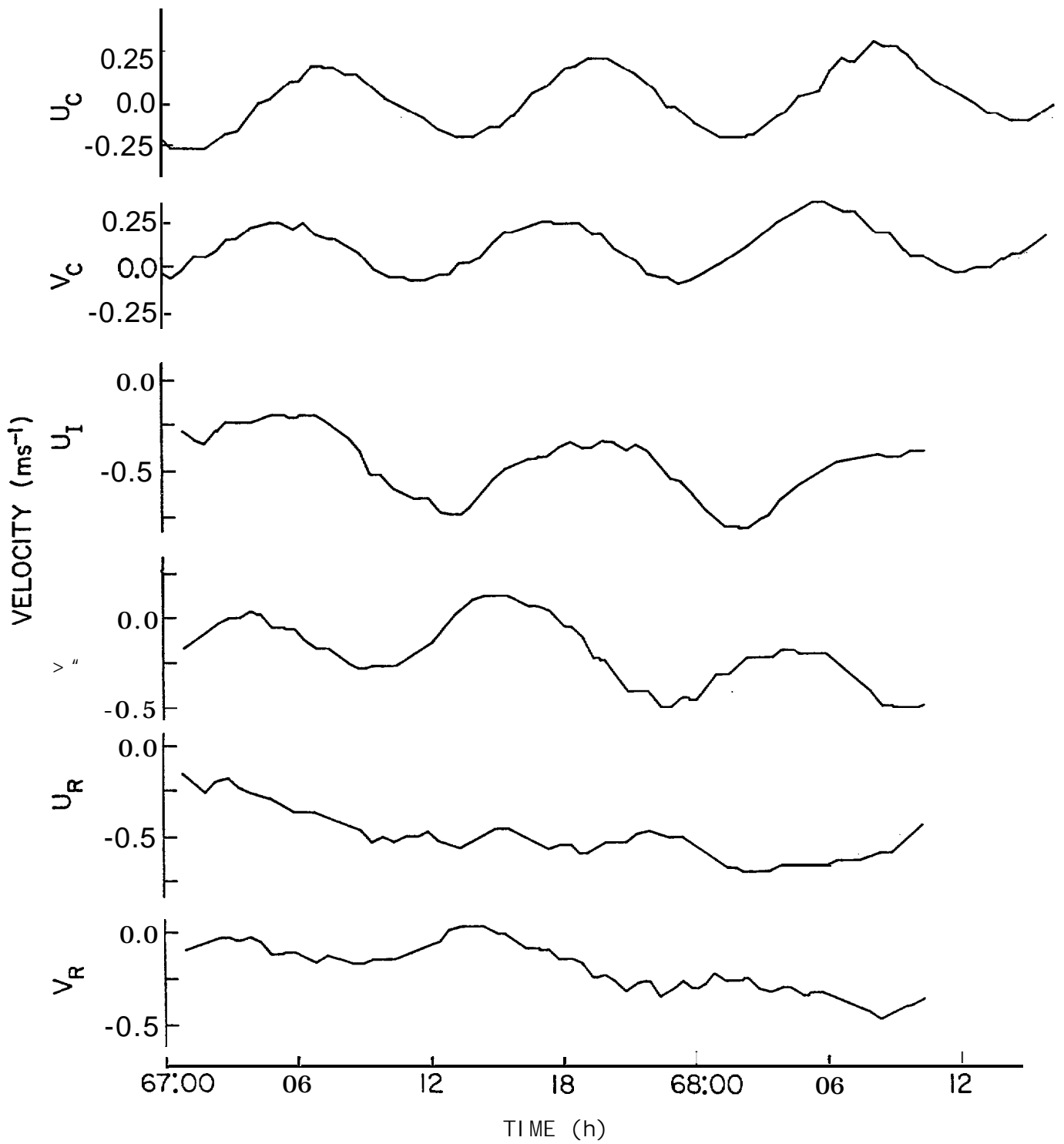


Figure 4. Comparison of band motion with currents measured at BC22.

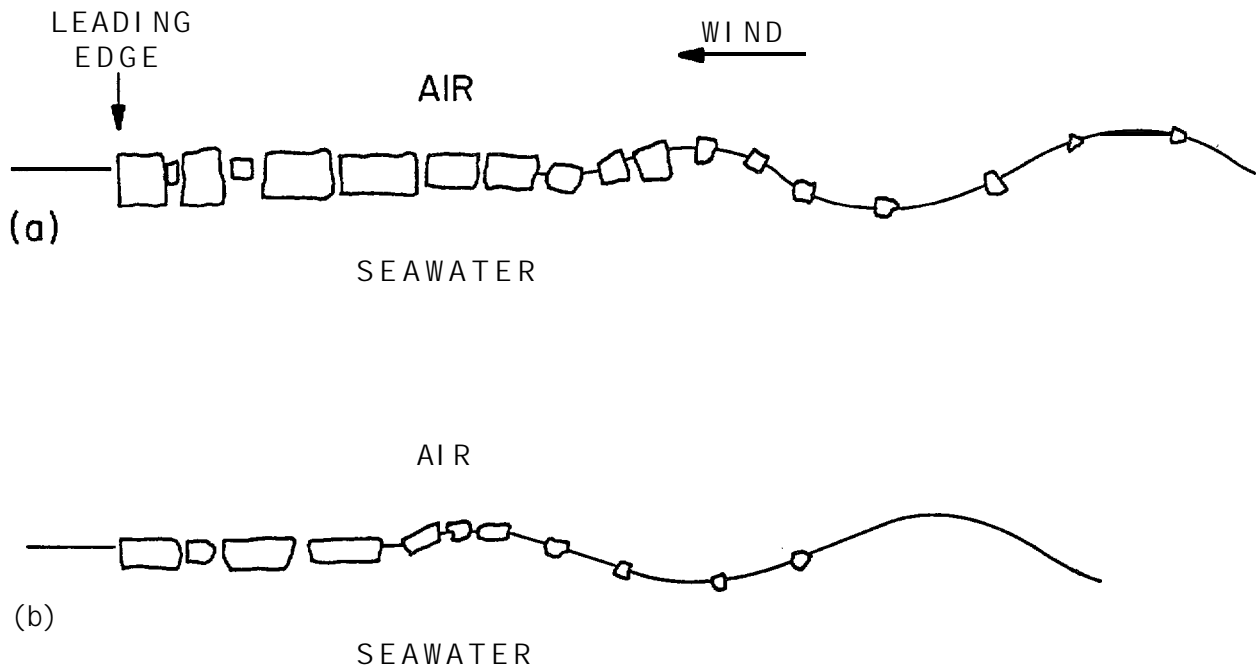


Figure 5. Schematic drawing of the band in cross section.

the surrounding warm water associated with the front. Although the ice also melts below, our field experiment suggests that the lateral erosion rate of the band is about 20 m hr^{-1} , or 0.5 km dy^{-1} . Third, Appendix 2 shows from a momentum balance on the band that the wave radiation stress, which is that stress exerted by the absorption and reflection of waves from the band, is the cause of the band acceleration relative to Pease's interior station.

Fourth, the Appendix also shows that the mean band motion can be modelled by a momentum balance among the air, water, Coriolis, and wave radiation stresses acting on the band. We also indirectly show that the AIDJEX water drag formulation is too large to describe the band motion; a better drag formulation is to use McPhee's (1982) sixth drag law described in Appendix 2.

Therefore, the physics of the ice response to wind and currents is very different in the MIZ than in the ice interior. There are three reasons for this .

1. Once the ice bands form, the internal ice stress term is unimportant.
2. The radiation stress term, which is the excess wave momentum flux exerted on the ice by the wind-waves generated in the fetch between the band and the next upwind obstacle, becomes on the same order as the wind stress.
3. The water stress term as described in the AIDJEX model is too large for the observed range of band velocities ($0.4 - 0.6 \text{ m s}^{-1}$). A better water drag formulation is McPhee's sixth drag law. The use of the AIDJEX drag in calculation of the band motion yields 20% slower band velocities than the McPhee law.

The use of this new information will permit modelling of these ice edge features.

4. Oil in the **MIZ**

When considering the presence of oil in the MIZ, our most important observations are as follows: The oceanography of the region is characterized by a nearly stationary front, which responds to storms through a sharpening of the **pycnocline**. This front has a temperature transition of **about** 5 deg over 100 km, so that the front should be clearly visible on the high resolution **IR** channel on the TIROS satellite. Since the location of this front determines the ice edge position, we should be able to tell from satellite observations where an oil spill will melt out.

Second, the above observations on band translation and decay give us further information on oil impact in the **MIZ**. We have already discussed in earlier reports the translation of oil south from Norton Sound within large floes, and that as these floes approach the **MIZ**, the incident waves fracture, raft, and ridge them into small, thick, oily floes. Then, the formation of these floes into bands will lead to the translation of oil away from the ice edge. Just as the small floes lag behind the bands as the bands decay from the upwind edge, so will oil lag behind the bands as the floes containing oil break up and melt. Therefore, the bands will leave a trail of oil sheen and slick, depending on the amount of entrained oil. Finally, an oil slick within the frontal region **will** be overrun by the bands, and thus transported at a greater speed until the bands melt away.